RPA: Tool for Rocket Propulsion Analysis

Assessment of Delivered Performance of Thrust Chamber

Alexander Ponomarenko

contact@propulsion-analysis.com

http://www.propulsion-analysis.com

March 2013 (v.1)

Abstract

Rocket Propulsion Analysis (RPA) is a multi-platform analysis tool intended for use in conceptual and preliminary design (design phases 0/A/B1).

This report describes a numerical models and computation techniques implemented in RPA to estimate the delivered performance of thrust chambers.

Contents

Nomenclature....3
Introduction....4
Numerical Model....4
Delivered Performance....4
Correction Factors....6
Finite Rate Kinetics in the Combustion Chamber....6
Boundary Layer (Friction) Loss....7
Divergence Loss....10
Multi-Phase Flow Loss....12
Built-In Assessment....13
Finite Rate Kinetics in the Nozzle....13
Finite-Area Combustion Chamber....13
Interzonal Losses....15
Nozzle Flow Separation....16
Thrust Throttling 17
Application in RPA and RPA SDK....19
References....20

Nomenclature

A	cross-sectional area, m^2
$\bar{A}$	relative cross-sectional area, $\bar{A} = A / A_t$
$\bar{F}$	specific cross-sectional area, $\bar{F} = A / \dot{m}$, $(s \cdot m^2)/kg$
c^*	characteristic velocity, m/s
I_s	specific impulse, m/s
C_f	thrust coefficient
p	pressure, Pa
T	temperature, K
w	velocity, m/s
M	Mach number
λ	characteristic Mach number
ρ	density, kg/m^3
$\dot{m}$	mass flow rate, kg/s
Re	Reynolds number
δ^{**}	boundary layer momentum thickness
η	dynamic viscosity, $kg/(m \cdot s)$
ξ	performance loss coefficient
ζ	performance correction factor, $\zeta = 1 - \xi$

Further symbols will be introduced and explained in the text.

Introduction

A number of computer codes can calculate ideal theoretical performance parameters of thrust chamber, usually providing overestimated specific impulse. In turn, this leads to overestimating of the overall performance, when ideal theoretical performance is used as input data for evaluating the expected parameters of the system. To compensate this issue, the correction factors have to be applied to the ideal performance parameters.

This report provides detailed information about semiempirical correction factors and computation techniques used in RPA to estimate the delivered performance of thrust chamber from calculated theoretical performance values with accuracy sufficient for conceptual and preliminary design studies, as well as for rapid evaluation of different variants of the systems.

Numerical Model

Delivered Performance

Thrust chambers performance calculated from thermodynamic analysis (see reference [1]) is an ideal theoretical performance and obtained under following assumptions: adiabatic, isenthalpic combustion with infinitely fast chemical reactions; adiabatic, isentropic (frictionless and no dissipative losses) quasi-one-dimensional nozzle flow; ideal gas law; no dissipative losses.

The performance parameters obtained from such analysis are:

- ideal specific impulse in vacuum I_s^{vac}
- ideal specific impulse at optimum expansion I_s^{opt}
- ideal specific impulse at sea level I_s^{SL}
- ideal thrust coefficient in vacuum C_f^{vac}
- ideal thrust coefficient at optimum expansion C_f^{opt}
- ideal thrust coefficient at sea level C_f^{SL}
- ideal characteristic velocity c^*

In the real thrust chambers the flow is axisymmetric two-dimensional (or even tree-dimensional), with a viscous boundary layer next to the nozzle walls, where the gas velocities are much lower than the the core-stream velocities, finite-rate chemical kinetics, and other factors which reduce the real delivered performance.

The deviations from ideal performance can be broken down into two classes:

- those that can be characterized by correction factors to be applied to calculated ideal performance parameters listed above
- and those that can be applied through modification of calculation of ideal performance parameters leading to deviations to be incorporated into performance parameters directly (“built-in assessment”)

Corrections factors can be grouped into two categories:

- combustion chamber correction factor ζ_c to correct the performance parameters due to real processes in the combustion chamber
- nozzle correction factor ζ_n to correct the performance parameters due to real processes in the nozzle

Corrections factors are given by:

$$\zeta_c = \zeta_r \tag{1}$$

$$\zeta_n = \zeta_f \zeta_d \zeta_z \tag{2}$$

where

ζ_r – correction factor that represents performance loss due to finite rate kinetics in the combustion chamber

ζ_f – correction factor that represents performance loss due to friction in boundary layer

ζ_d – correction factor that represents performance loss due to divergence, or two-dimensional flow in the nozzle

ζ_z – correction factor that represents performance loss due to multi-phase flow in the nozzle

Using introduced correction factors, the assessment of delivered performance parameters can be performed as follows:

$$\left(I_s^{vac}\right)_d = \zeta_c \zeta_n I_s^{vac} \tag{3}$$

$$\left(I_s^{opt}\right)_d = \zeta_c \zeta_n I_s^{vac} - \bar{F}_e p_e = \left(I_s^{vac}\right)_d - \bar{F}_e p_e \tag{4}$$

$$\left(I_s^{SL}\right)_d = \zeta_c \zeta_n I_s^{vac} - \bar{F}_e p_a^{SL} = \left(I_s^{vac}\right)_d - \bar{F}_e p_a^{SL} \tag{5}$$

$$\left(c^*\right)_d = \zeta_c c^* \tag{6}$$

$$\left(C_f^{vac}\right)_d = \frac{\left(I_s^{vac}\right)_d}{\left(c^*\right)_d} = \zeta_n C_f^{vac} \tag{7}$$

$$\left(C_f^{opt}\right)_d = \frac{\left(I_s^{opt}\right)_d}{\left(c^*\right)_d} = \zeta_n C_f^{opt} \tag{8}$$

$$\left(C_f^{SL}\right)_d = \frac{\left(I_s^{SL}\right)_d}{\left(c^*\right)_d} = \zeta_n C_f^{SL} \tag{9}$$

where $\bar{F}_e = A_e / \dot{m} = 1/\left(w\rho\right)_e$ is a nozzle exit specific area.

Built-in assessment include the following performance losses:

- loss due to stagnation pressure drop in finite-area combustion chamber
- loss due to finite rate kinetics in the nozzle
- interzonal losses due to deviation of parameters in the core-stream and boundary layer with injected coolant (BLC)
- loss due to nozzle flow separation

– loss due to trust throttling.

Correction Factors

Finite Rate Kinetics in the Combustion Chamber

The correction factor that represents performance loss due to finite rate kinetics in the combustion chamber with accuracy sufficient for conceptual and preliminary design studies is calculated as:

$$\zeta_r = (1-\xi_r^{'})(1-\xi_r^{''}) \quad (10)$$

The therm $\xi_r^{'}$ can be estimated using empirical function [8]:

$$\xi_r^{'} = \left(\frac{h_0}{r_t}\right)^a \left(\frac{p_{SL}}{p_c}\right)^b \log_{10}\left(\frac{r_e}{r_t}\right) \quad (11)$$

where

p_{SL} – ambient pressure at sea level

p_c – chamber pressure

r_t – nozzle throat radius

r_e – nozzle exit radius

Parameters h_0 , *a* and *b* for several propellant composition are given in following table [8]:

Propellant	***Oxidizer excess coefficient***	h_0 ***, m***	***a***	***b***
O_2+H_2	0.8	$1.3\cdot10^{-3}$	0.4	1
O_2+kerosine	0.8	$6.7\cdot10^{-4}$	0.35	0.8
AT+UDMH	0.9	$5.3\cdot10^{-6}$	0.25	0.5

For quick estimation the performance loss $\xi_r^{'}$ can also be obtained from the following diagram:

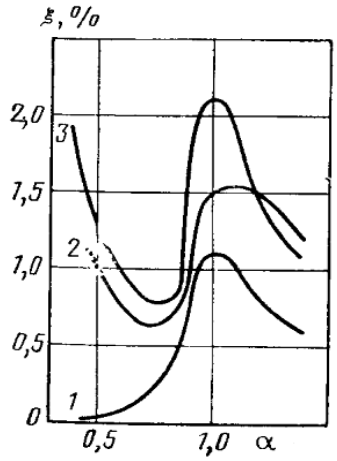

Figure 1: Performance loss coefficient $\xi_r^{'}$ (taken from [3])

Here α is an oxidizer excess coefficient, curves 1, 2 and 3 represent losses for propellants O_2+H_2, F_2+H_2 and AT+UDMH correspondingly.

The therm $\xi_r^{'}$ represents the increase in loss for low-pressure combustion chambers and is given by:

$$\xi_r^{''} = max\left[0,\ \frac{2.1-\ln\left(p_c/(2\cdot 10^6)\right)}{100}\right] \tag{12}$$

where p_c is a combustion chamber pressure [Pa].

Boundary Layer (Friction) Loss

The correction factor due to wall friction in boundary layer can be calculated using following relation [3,7]:

$$\zeta_f = 1 - \frac{2\bar{\delta}_e^{**}}{1 + \frac{1}{k M_e^2}} \tag{13}$$

where

$\bar{\delta}_e^{**} = \delta^{**}/r_e$ – relative momentum thickness

r_e – nozzle exit radius

M_e – Mach number at nozzle exit obtained for quasi two-dimensional nozzle flow

k – specific heats ratio

This expression is applicable both for laminar and turbulent boundary layers.

In rocket engine nozzles the boundary layer is usually laminar at $\mathrm{Re}_{w_0}<1\cdot10^7$ and turbulent at $\mathrm{Re}_{w_0}>3\cdot10^7$. Here Reynolds number is given by:

$$\mathrm{Re}_{w_0} = \frac{w_e \rho_{0c} L_n}{\eta_w}$$

w_e – gas exhaust velocity in vacuum

ρ_{0c} – gas stagnation density at nozzle inlet

L_n – nozzle length

η_w – dynamic viscosity at T_w

Smaller engines (with thrust below 45000 N) tend to have laminar boundary layers, whereas the large engines are almost always turbulent [6].

For turbulent boundary layer the momentum thickness δ^{**} is given by [3]:

$$\delta^{**} = \frac{\left(\frac{2}{k-1}\right)^{0.1}}{\mathrm{Re}_{w_0}^{0.2}} \left(\frac{0.015}{\bar{T}_w^{0.5}}\right)^{0.8} \frac{\left(1+\frac{k-1}{2}M_{we}^2\right)^{\frac{k+1}{2(k-1)}}}{M_w^{\nu+1}} \frac{\bar{S}^{0.2}}{\bar{r}_e^2} \left[\int_0^{\bar{S}} \frac{\bar{r}^{1.25} M^{1+1.25\nu}}{\left(1+\frac{k-1}{2}M_w^2\right)^{\frac{1.36k-0.36}{k-1}}} d\bar{S}\right]^{0.8} \qquad (14)$$

where

$\bar{T}_w = \frac{T_w}{T_0}$, for adiabatic nozzles $\bar{T}_w=0.9$

$\nu = \frac{18}{7}\bar{T}_w - \frac{2}{7}$

T_w – nozzle wall temperature

T_0 – gas stagnation temperature

M_w – Mach number next to the nozzle wall

M_{we} – Mach number at nozzle exit next to the nozzle wall

$\bar{S} = \frac{S}{r_t}$ – relative lateral length of nozzle

r_t – nozzle throat radius

This equation can be used both for convergent and divergent nozzle sections.

For laminar boundary layer the momentum thickness δ^{**} can be calculated using equations 18.23 – 18.25 in [4].

For nozzle with know distribution of viscosity stress along the contour (this is usually the case if thermal analysis of the chamber is performed), the correction factor due for friction in boundary layer can be calculated using following relation [2,10]:

$$\zeta_f = 1 - \frac{2\pi \int_0^{x_e} \tau R \cos\theta \, dx}{C_f A_t p_{0c}} \tag{15}$$

where

ζ_f – performance correction factor for the friction loss

τ – viscosity stress (see section “Gas-Side Heat Transfer” in reference [2])

C_f – ideal thrust coefficient

A_t – nozzle throat area

p_{0c} – stagnation pressure at nozzle inlet

x , R , θ – size and shape parameters of the thrust chamber as defined in Figure 1 in reference [2].

For quick estimation the performance loss can be estimated using the following diagram:

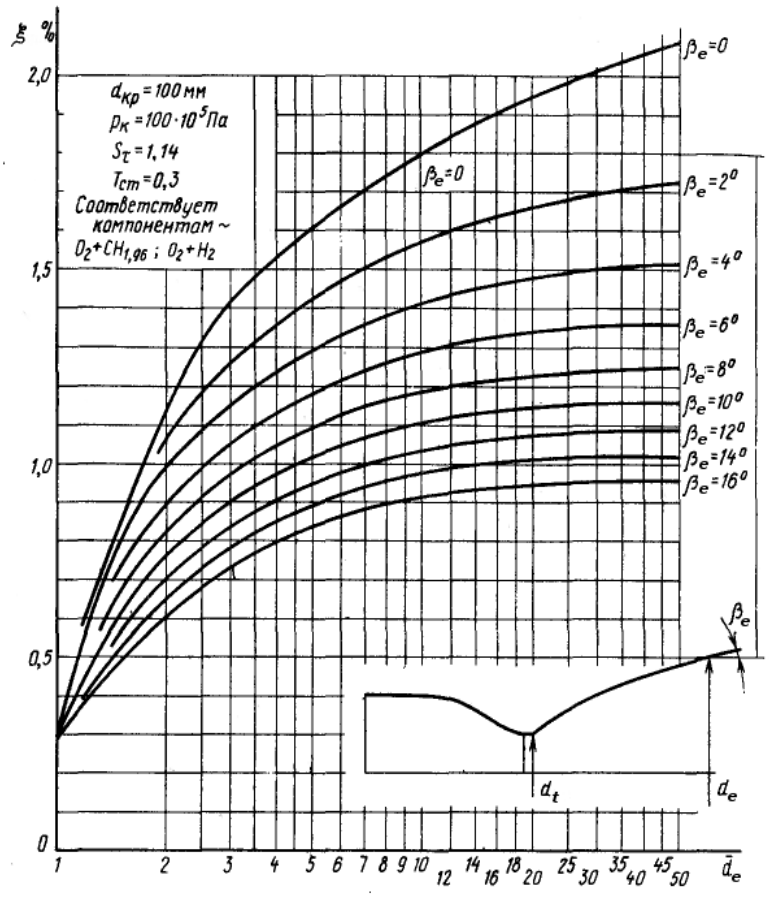

Figure 2: Performance loss coefficient due to friction in boundary layer (taken from [5])

Divergence Loss

For conical nozzle the correction factor is given by following equation [9]:

$$\zeta_d = \frac{1+\cos\theta_e}{2} \tag{16}$$

where

θ_e – half-angle of the conical nozzle.

For bell nozzles with known pressure field distribution at nozzle exit the correction factor for divergence loss can be calculated using the equation [3]:

$$\zeta_d = 1 - \frac{\left(\frac{2}{k+1}\right)^{\frac{1}{k-1}} \left[z(\lambda_e)-1\right] - \bar{P}}{\left(\frac{2}{k+1}\right)^{\frac{1}{k-1}} z(\lambda_e)} \tag{17}$$

where

$z(\lambda_e) = 0.5(\lambda_e + 1/\lambda_e)$

λ_e – characteristic Mach number at nozzle exit obtained for quasi two-dimensional nozzle flow

$$\bar{P} = \int_1^{\bar{r}_e} \frac{p}{p_{0c}} \bar{r}\, d\bar{r}$$

$\bar{r} = r/r_t$ – nozzle exit relative radius

k – specific heats ratio

For bell nozzles with known gas velocity field distribution at nozzle exit the correction factor for divergence loss can be calculated as follows [5]:

$$\zeta_d = \frac{(C_f^{vac})_{2D}}{(C_f^{vac})_{1D}} \tag{18}$$

where

$(C_f^{vac})_{1D}$ – thrust coefficient calculated for quasi-one-dimensional nozzle flow

$(C_f^{vac})_{2D}$ – thrust coefficient calculated for axisymmetric two-dimensional nozzle flow given as:

$$(C_f^{vac})_{2D} = 2\frac{A_e}{A_t}\int_0^1 \left(1-\frac{k-1}{k+1}\lambda^2\right)^{\frac{1}{k-1}} \left[1+\lambda^2\frac{k(2\cos^2\beta-1)+1}{k+1}\right] \bar{r}\, d\bar{r} \tag{19}$$

where

λ – characteristic Mach number at nozzle exit (see Figure 3).

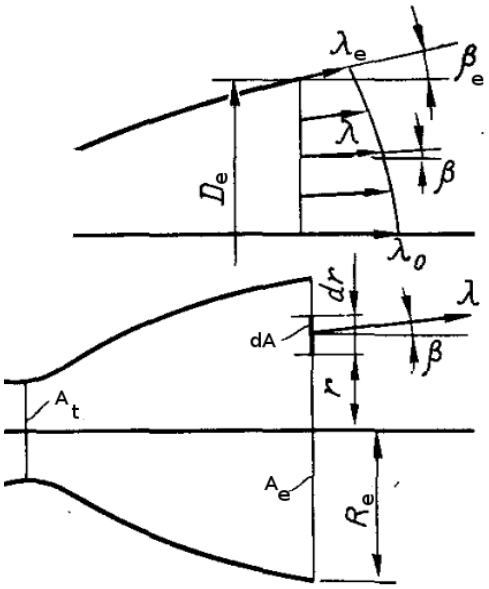

Figure 3: Velocity field distribution at nozzle exit (taken from [5])

Alternatively, the correction factor for bell nozzle can be estimated using the following empirical equation [4]:

$$\zeta_d = 1 - B\frac{e^{n\left(1-\frac{\bar{r}_e}{\bar{r}_0}\right)} - 1}{e^n - 1} \tag{20}$$

where

$B = 1.52\left(\exp[-30(k-1)]+0.1\right)$

$n = 1.45\,\bar{r}_0^{0.25} - 0.005\,\bar{r}_0$

$\bar{r}_0 = 1 + \frac{\bar{r}_e - 1}{\bar{L}}$

$\bar{r}_e = r_e / r_t$ – nozzle exit relative radius

$\bar{L}$ – relative nozzle length

$k = \ln(p_{0c}/p_e)/\ln\left(\frac{p_{0c}}{p_e}\frac{(RT)_e}{(RT)_{0c}}\right)$ – average isentropic expansion coefficient

This equation is applicable for nozzles with $\bar{L} = (0.4 \ldots 1.0)$ and $k = (1.1 \ldots 1.25)$.

For quick estimation the correction factor can also be obtained from the following diagram:

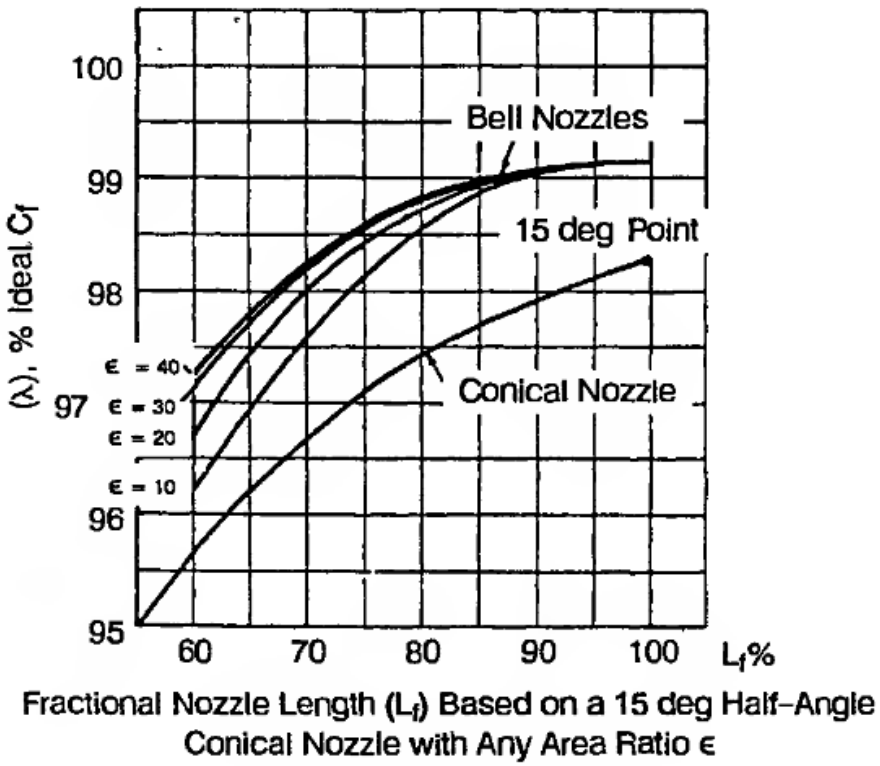

Figure 4: Thrust efficiency vs bell nozzle length (taken from [9])

Multi-Phase Flow Loss

Correction factor is calculated from following relations derived from relations given in reference [9]:

$$\zeta_z = 0.2\zeta_{zw} + 0.8\zeta_{zT} \tag{21}$$

$$\zeta_{zw} = 1 - \frac{Z C_s}{w_e^2}\left[T_c - T_e\left(1 + \ln\frac{T_c}{T_e}\right)\right] \tag{22}$$

$$\zeta_{zT} = 1 - \frac{Z}{2} \tag{23}$$

where

Z – mass fraction of condensed phase at nozzle exit

C_s – specific heat capacity of condensed phase

w_e – gas velocity at nozzle exit

T_e – gas temperature at nozzle exit

T_c – gas temperature at combustion chamber

Built-In Assessment

Finite Rate Kinetics in the Nozzle

For analysis of chemical equilibrium during nozzle expansion the following models can be used [16]:

1. Frozen equilibrium with no change in gas composition. This approach usually gives low performance.
2. Shifting equilibrium or instantaneous change in composition. This approach usually overrates the performance slightly.
3. Suddenly frozen flow, which is a combination of the first two models: shifting equilibrium is applied for analysis of chemical equilibrium from combustion chamber injector face to some station of the nozzle ("frozen station") where the analysis method is replaced with frozen equilibrium model that is applied from the mentioned nozzle station to the nozzle exit. Nozzle station is defined either by pressure ratio or area ratio.

The values of I_s and C_f obtained from suddenly frozen flow analysis usually are between those of frozen and instantaneously shifting equilibria. Therefore the model of suddenly frozen flow can be used to estimate the chamber performance with accuracy sufficient for conceptual and preliminary design.

The following empirical values of area ratio A_{fr}/A_t can be used to define the "frozen station" downstream of the nozzle throat for different propellants:

	LOX+Kerosene LOX+Alcohol	LOX+LH2	N_2O_4+UDMH
A_{fr}/A_t	1.3	3	6

Finite-Area Combustion Chamber

When the combustion chamber has a cross section that is larger than about four times the throat area ($\bar{A}_c = A_c/A_t > 4$), the gas velocity in the chamber can usually be neglected. To the contrary, in combustion chambers with relatively small cross section, the expansion of the gases is accompanied by significant acceleration and pressure drop. The acceleration process in the chamber is assumed to be adiabatic, but not isentropic, and the pressure drop leads to the lower pressure at nozzle inlet p_c . This causes a small loss in specific impulse.

The method of calculation of stagnation pressure drop at the nozzle inlet is given in reference [1] and reproduced below.

Because both nozzle inlet pressure p_c and nozzle throat pressure p_t are unknown, two-level iterative procedure is conducted with initial estimates

$$p_c^{(0)} = \frac{1}{\pi(\lambda_c)\left[1+\frac{k_{inj} M_c^2}{(\beta_T p)_{inj}}\right]} \tag{24}$$

where λ_c is a characteristic Mach number at nozzle inlet obtained for subsonic flow from equation [9]

$$\frac{1}{\bar{A}_c} = \left(\frac{k+1}{2}\right)^{\frac{1}{k-1}} \lambda_c \left(1-\frac{k-1}{k+1}\lambda_c^2\right)^{\frac{1}{k-1}} \tag{25}$$

with assumption $k = k_{inj}$; M_c is a Mach number that corresponds to the calculated characteristic Mach number;

$$\beta_T = -\frac{\left(\frac{\delta \ln V}{\delta \ln p}\right)_T}{p} \tag{26}$$

and

$$\pi(\lambda_c) = \left(1-\frac{k-1}{k+1}\lambda_c^2\right)^{\frac{k}{k-1}} \tag{27}$$

also with assumption $k = k_{inj}$;

$$\rho_c^{(0)} = \rho_{inj} \tag{28}$$

For the assigned chamber contraction area ratio $\bar{A}_c = A_c / A_t$, the iteration proceeds as follows:

1. Assuming that velocity at injector face can be neglected, the velocity at the nozzle inlet is obtained from the momentum equation for steady one-dimensional flow:

$$w_c^{(i)} = \sqrt{\frac{p_{inj} - p_c^{(i)}}{\rho_c^{(i)}}} \tag{29}$$

2. If acceleration process in the chamber is adiabatic, the total enthalpy per unit mass is constant. Recalling that velocity at injector face can be neglected, the specific enthalpy at nozzle inlet can be expressed as

$$h_c^{(i)} = h_{inj} - \frac{(w_c^{(i)})^2}{2} \tag{30}$$

3. Solution of the problem *(p,H)$_c$=const* for the nozzle inlet section provides the entropy at nozzle inlet $S_c^{(i)}$.

4. Known conditions at nozzle inlet and assumption about an isentropic expansion in the nozzle allow to obtain the throat conditions (including throat pressure $p_t^{(i)}$ and density $\rho_t^{(i)}$), utilizing the procedure similar to that for the infinite-area combustion chamber (equations 47 to 50 in [1]).

5. From the continuity equation for steady quasi-one-dimensional flow, find the velocity at the

nozzle inlet for the specified chamber contraction ratio:

$$\breve{w}_c = \left(\frac{\rho_t w_t}{\rho_c} \right)^{(i)} \frac{1}{\bar{A}_c} \tag{31}$$

6. From the momentum equation, find the pressure at injector face that corresponds to the calculated pressure and velocity at the nozzle inlet:

$$\breve{p}_{inj} = p_c^{(i)} + \rho_c^{(i)} \breve{w}_c^2 \tag{32}$$

7. Repeat steps 1 to 6 until the relative deviation of pressure at injector face is within required convergence tolerance:

$$\frac{|p_{inj} - \breve{p}_{inj}|}{p_{inj}} < \varepsilon \tag{33}$$

The improved nozzle inlet pressure for the next iteration *(i+1)* is calculated as

$$p_c^{(i+1)} = p_c^{(i)} \frac{p_{inj}}{\breve{p}_{inj}} \tag{34}$$

The stagnation pressure at nozzle inlet section can be computed from

$$p_{0c} = p_c \left[1 + (k_c - 1) \frac{w_c^2 \rho_c}{2 k_c p_c} \right]^{\frac{k_c}{k_c - 1}} \tag{35}$$

Interzonal Losses

Relatively cold layer next to the chamber walls can be used for thermal protection of the chamber. Such layer is usually generated by injection of the fuel (or oxidizer) in excess through the peripheral injector elements or special holes/slots in the wall.

The influence of shear flow with interzonal variations of mixture ratio on the chamber performance is estimated under following assumptions:

- the large-scale distribution of mixture ratio and the gas properties in the shear flow are conserved along the nozzle
- pressure is constant in any point of chamber cross-section at any location
- in any point of nozzle throat section the Mach number M=1.

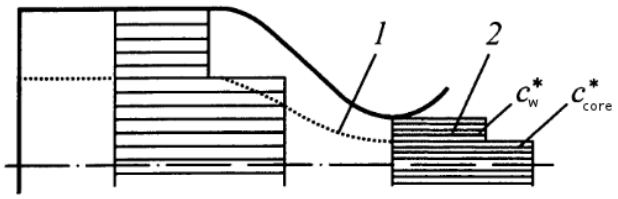

Figure 5: Shear flow in the nozzle

The following equations for ideal chamber performance can be derived using mentioned assumptions [6,9]:

$$I_s = (1-\bar{m}_w)(I_s)_{core} + \bar{m}_w (I_s)_w \quad (36)$$

$$c^* = (1-\bar{m}_w) c^*_{core} + \bar{m}_w c^*_w \quad (37)$$

$$C_f = \frac{I_s}{c^*} \quad (38)$$

where

$(I_s)_{core}$, c^*_{core} – ideal specific impulse and ideal characteristic velocity correspondingly, both calculated for design mixture ratio in the core flow

$(I_s)_w$, c^*_w – ideal specific impulse and ideal characteristic velocity correspondingly, both calculated for mixture ratio with excess of the fuel in the wall layer

$\bar{m}_w = \dot{m}_w / \dot{m}$ – relative mass flow rate through the wall layer

$\dot{m}$ – total mass flow through the chamber

The first equation can be used for calculation of ideal specific impulse at any ambient conditions (vacuum, optimal expansion and sea level), if corresponding values for $(I_s)_{core}$ and $(I_s)_w$ are used.

Nozzle Flow Separation

The theoretical prediction of free shock separation has been extensively studied in the past. In strongly overexpanding nozzles, the flow separates from the wall at a certain pressure ratio of wall pressure to ambient pressure p_i / p_a . Thy typical structure of the flowfield near the separation point i for the free shock separation is shown in Figure 6.

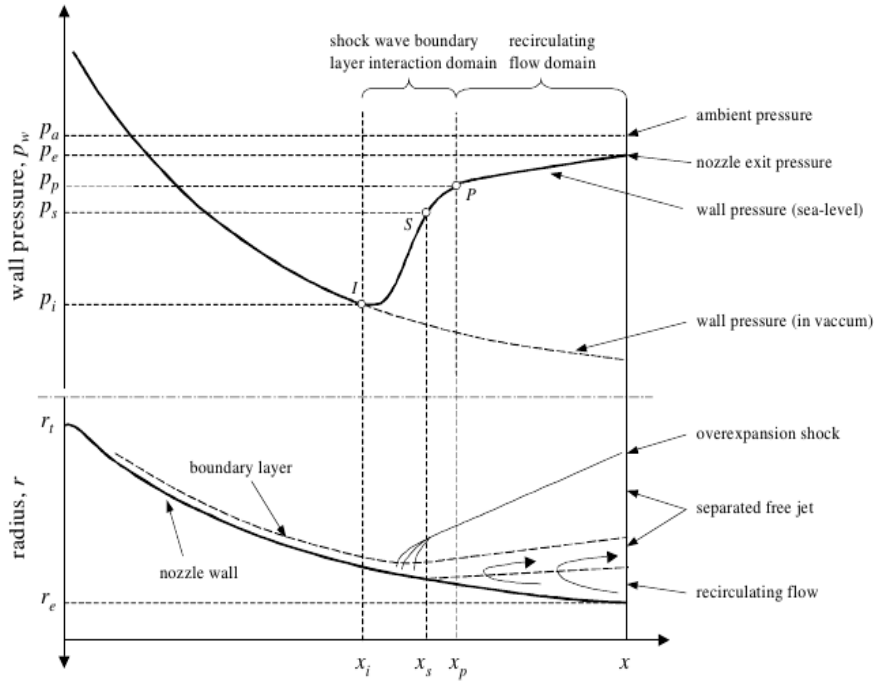

Figure 6: Phenomenological sketch of free shock separation (taken from [12])

Experimental data have been used to develop a number of empirical and semi-empirical criteria (many of them presented in compact form in reference [14]) in order to give the nozzle designer a prediction tool for the separation point (x_i on Figure 6), although knowing that in reality there is no exact point of separation.

In RPA, the following empirical separation criterion proposed by Schmucker [13] is used:

$$\frac{p_i}{p_a} = (1.88\,M_i - 1)^{-0.64} \tag{39}$$

where

p_i – wall pressure at the separation point i

p_a – ambient pressure

M_i – Mach number from the beginning of the separation zone

Simplistic approach to calculate chamber performance with flow separation can be described as follows:

Criterion of flow separation in the nozzle is given by:

$$(p_a)_{crit} = \frac{p_e}{(1.88\,M_e - 1)^{-0.64}} \tag{40}$$

Flow separation in the nozzle may only occur if $p_a > (p_a)_{crit}$.

The nozzle station i where flow separation occurs is defined by pressure p_i :

$$p_i = p_a(1.88\,M_i - 1)^{-0.64} \tag{41}$$

The chamber performance equations are derived from relations taken from [15]:

$$I_s = (I_s)_i + \Delta p(\bar{F}_i - \bar{F}_e) \tag{42}$$

where

$(I_s)_i = (I_s^{vac})_i - \bar{F}_i\,p_a$ – performance of the nozzle truncated to station i at given ambient pressure p_a

$\Delta p = \eta(p_a - p_i)$

$\eta = 0.1 \ldots 0.5$ – coefficient of pressure recovery downstream of station i

$\bar{F}_{\mathrm{i,e}} = \frac{1}{(w\rho)_{\mathrm{i,e}}}$ – specific area at stations i or e correspondingly

Thrust Throttling

Since chamber thrust is directly proportional to the mass flow rate, chambers are throttled by controlling the propellant mass flow rate $\dot{m}$. The reduced mass flow will cause an almost linear decrease in chamber pressure and thus almost linear decrease of thrust. The specific impulse would would also decrease slightly. Thus, there is a small performance penalty for throttling the thrust [16].

When the combustion chamber has a cross section that is larger than about 10 times the throat area ($\bar{A}_c = A_c / A_t > 10$), the non-linearity of decrease in pressure due to reduced mass

flow can be neglected. In this case the performance penalty is caused by lower temperature in combustion chamber. The chamber performance is calculated directly for combustion chamber pressure $p_c = r(p_c)_n$. Here subscript n designates parameters for the nominal thrust, and r is a throttle value defined as $r = \dot{m}_n / \dot{m}$ ($r = 1$ for nominal thrust).

For nozzle with fixed geometry, the lower combustion chamber pressure leads to the lower nozzle exit pressure, which in turn may cause the nozzle flow separation due to lower value of $(p_a)_{crit}$. In this case the performance is assessed as described in chapter *Nozzle Flow Separation*.

In combustion chambers with relatively small cross section, non-linear relation between mass flow rate and chamber pressure will cause larger decrease in chamber pressure for the same change of mass flow rate.

The method of calculation of combustion chamber pressure for specified throttle value r is given below.

For known combustion chamber contraction area ratio $\bar{A}_c = A_c / A_t$ and combustion chamber mass flux at nominal thrust $(\bar{m}_c)_n = \dot{m}_n / A_c = 1/\bar{F}_c = (w\rho)_c^n$, the iteration for given throttle value r proceeds as follows:

1. Initial estimation of pressure at injector face:

$$p_{inj}^{(0)} = r(p_{inj}^{(0)})_n \tag{43}$$

   where $(p_{inj}^{(0)})_n$ is the pressure at injector face at nominal thrust, obtained as described in chapter *Finite-Area Combustion Chamber.*

2. Using procedure for the finite-area combustion chamber described in chapter *Finite-Area Combustion Chamber*, obtain conditions at the nozzle inlet for the given chamber contraction ratio $\bar{A}_c$ and current value of pressure at injector face $p_{inj}^{(i)}$ (*i* is an iteration counter).

3. Calculate combustion chamber mass flux as:

$$\bar{m}_c^{(i)} = (w\rho)_c^{(i)} \tag{44}$$

4. Repeat steps *2* and *3* until the relative deviation of mass flux is within required convergence tolerance:

$$\left| 1 - \frac{\bar{m}_c^{(i)}}{r\,\bar{m}_{nc}} \right| < \varepsilon \tag{45}$$

   For each next iteration *(i+1)* calculate an improved chamber pressure as:

$$p_{inj}^{(i+1)} = p_{inj}^{(i)} \left(2 - \frac{\bar{m}_c^{(i)}}{r\,\bar{m}_{nc}} \right) \tag{46}$$

Using obtained final value of pressure at injector face $p_{inj}^{(final)}$, calculate conditions at nozzle inlet, nozzle throat and nozzle exit sections, as well as theoretical chamber performance.

Application in RPA and RPA SDK

Described methods for estimation of performance losses are used in RPA in following modules:

1. Thermodynamic analysis and thrust chamber performance prediction
    - performance loss due finite rate kinetics in combustion chamber is estimated using relations 10, 12 and digitized data obtained from Figure 1
    - divergence loss is estimated using relation 16 and digitized data obtained from Figure 4
    - multi-phase flow loss is estimated using relations 21, 22 and 23
    - performance loss due finite rate kinetics in the nozzle is estimated using model of suddenly frozen flow as described in corresponding chapter
    - performance loss due to finite-area combustion area is estimated as described in corresponding chapter
    - performance change due to nozzle flow separation is estimated as described in corresponding chapter
    - performance change due to thrust throttling is estimated as described in corresponding chapter
2. Thrust chamber sizing and design of nozzle contour
    - when designing the truncated ideal contour (TIC) using axisymmetric two-dimensional method of characteristic, divergence loss is estimated using relations 18 and 19, and boundary layer (friction) loss is estimated using relations 13 and 14
3. Thrust chamber thermal analysis
    - when performing thermal analysis using Ievlev's approach, boundary layer (friction) loss is estimated using relation 15

In addition to that, RPA Software Development Kit (SDK) provides API functions for estimation of interzonal losses due to deviation of parameters in the core-stream and boundary layer with injected coolant (BLC) as described in chapter *Interzonal Losses*.

References

1. Ponomarenko A. RPA: Tool for Liquid Propellant Rocket Engine Analysis. 2010.

2. Ponomarenko A. RPA: Tool for Rocket Propulsion Analysis. Thermal Analysis of Thrust Chambers. 2012

3. Alemasov V.E., Dregalin A.F., Tishin A.P. Theory of Rocket Engines. Moscow, Mashinostroenie, 1980. (in Russian)

4. Glushko V.P., Alemasov V.E., et al. Thermodynamic and Thermophysical Properties of Combustion Products. Volume 1 – Moscow, USSR Academy of Science, 1971. (in Russian)

5. Vasiliev A.P., Kudryavtsev V.M. et al. Basics of theory and analysis of liquid-propellant rocket engines, vol.2. 4th Edition. Moscow, Vyschaja Schkola, 1993. (in Russian)

6. Douglas E. Coats. Assessment of Thrust Chamber Performance. Liquid Rocket Thrust Chambers - Aspects of Modeling, Analysis, and Design - Progress in Astronautics and Aeronautics, Volume 200.

7. Katorgin B.I., Kiselev A.S., Sternin L.E., Chvanov V.K. Applied gas dynamics. Moscow, Vusovskaja kniga, 2009. (in Russian)

8. Kozlov A.A., Novikov V.N., Solovjev E.V. Feed Systems and Control of Liquid-Propulsion Systems. Moscow, Mashinostroenie, 1988. (in Russian)

9. Dorofeev A.A. Fundamentals of thermal rocket engines. Theory, calculation and design. Moscow, Bauman MSTU, 2010. (in Russian)

10. Lebedinsky E.V., Kalmykov G.P., et al. Working processes in liquid-propellant rocket engine and their simulation. Moscow, Mashinostroenie, 2008. (in Russian)

11. Huzel, D.K., Hwang, D.H., Modern Engineering for Design of Liquid Rocket Engines, ISBN 1-56347-013-6, American Institute of Aeronautics and Astronautics, 1992.

12. Jan Östlund. Flow processes in rocket engine nozzles with focus on flow separation and side-loads. Stockholm, 2002.

13. Schmucker, R. Flow Processes in Overexpanded Chemical Rocket Nozzles. Part 1: Flow Separation. NASA, Washington, 1984.

14. Ralf H. Stark. Flow Separation in Rocket Nozzles, a Simple Criteria. DLR, Germany, 2005. AIAA2005-3940.

15. Dobrovolsky M.B. Liquid-propellant rocket engines. Moscow, Bauman MSTU, 2005. (in Russian)

16. Sutton, G.P. and Biblarz, O. Rocket Propulsion Elements, 7th Edition. John Wiley & Sons, 2001.